JGR Space Physics

RESEARCH ARTICLE
10.1029/2023JA031454

Magnetospheric Line Radiation Observed Close to the Source: Properties and Propagation

F. Němec[1], J. Manninen[2], O. Santolík[1,3], G. B. Hospodarsky[4], and W. S. Kurth[4]

[1]Faculty of Mathematics and Physics, Charles University, Prague, Czech Republic, [2]Sodankylä Geophysical Observatory, Sodankylä, Finland, [3]Department of Space Physics, Institute of Atmospheric Physics of the Czech Academy of Sciences, Prague, Czech Republic, [4]Department of Physics and Astronomy, University of Iowa, Iowa City, IA, USA

Key Points:

- Van Allen Probes high-resolution burst mode data are searched for Magnetospheric Line Radiation (MLR) events, 15 events identified
- The Poynting flux is directed away from the equatorial plane, suggesting that the MLR is generated at the geomagnetic equator
- MLR frequency modulation is related to an electrostatic wave with frequency equal to the MLR frequency spacing

Correspondence to:
F. Němec,
frantisek.nemec@mff.cuni.cz

Citation:
Němec, F., Manninen, J., Santolík, O., Hospodarsky, G. B., & Kurth, W. S. (2023). Magnetospheric line radiation observed close to the source: Properties and propagation. *Journal of Geophysical Research: Space Physics*, *128*, e2023JA031454. https://doi.org/10.1029/2023JA031454

Received 2 MAR 2023
Accepted 22 MAY 2023

Abstract Magnetospheric Line Radiation (MLR) is a type of whistler mode electromagnetic wave phenomenon observed in the inner magnetosphere at frequencies of a few kilohertz, that is characterized by a frequency modulation of the wave intensity. Although such events are quite regularly observed by ground-based stations and low-altitude spacecraft, their observations in the equatorial region at larger radial distances (i.e., close to tentative source regions) are extremely limited, likely due to the generally low frequency resolution of available measurements. A systematic search for MLR in continuous intervals of high-resolution multicomponent wave data obtained by the Van Allen Probes spacecraft detects 15 events. They occur primarily on the dayside at frequencies between about 1 and 5 kHz, propagating with oblique wave normals away from the geomagnetic equator. For one event, simultaneous ground-based observations are available, providing limits on the spatial extent of the event: it does not extend beyond the high-density plasmasphere region. An electrostatic wave at a frequency corresponding to the modulation frequency of MLR is observed in three events. This is likely linked to the event formation mechanism and has not been observed before. Our results can lead to an understanding of the formation mechanism of MLR.

1. Introduction

The intensity of whistler mode electromagnetic waves observed in the Earth's inner magnetosphere at frequencies between about 1 and 8 kHz sometimes peaks at rather well defined equidistant frequencies. These frequencies may slowly change with time, and the corresponding frequency-time spectrograms are thus formed by a system of several equidistant intense lines, either constant in frequency or slowly drifting. Such events are generally called Line Radiation (LR). Two different basic types of LR can be distinguished (Němec et al., 2007a; Rodger et al., 1995).

One type of LR event is characterized by narrow spectral lines with a frequency separation corresponding to the base frequency of electric power systems. Such events, called Power Line Harmonic Radiation (PLHR), can be linked to electromagnetic radiation from electric power systems on the ground, and their formation and properties are reasonably understood (Němec et al., 2006, 2007b, 2008). The second type of event, with broader spectral lines and frequency spacing not corresponding to the power system frequency (Matthews & Yearby, 1981; Rodger et al., 1999), is called Magnetospheric Line Radiation (MLR). Although MLR events have been observed by ground-based stations (Manninen, 2005; Rodger et al., 2000a, 2000b) and satellites (Bell et al., 1982; Němec, Parrot, et al., 2009) for a few decades, their origin has not been yet adequately explained. It has been suggested that they might be generated by an interaction between a wave of a carrier frequency and an additional wave with a frequency equal to the MLR frequency spacing (Němec, Parrot, & Santolík, 2012).

During periods of enhanced geomagnetic activity, MLR events tend to be observed at lower L-shells (Bezděková et al., 2015), and their frequency spacing increases (Bezděková et al., 2019), possibly due to the movement of the source region to lower radial distances and related increase of characteristic frequencies. Simultaneous observations by three different spacecraft (Němec, Santolík, et al., 2012) and by a spacecraft and a ground-based station (Němec, Raita, et al., 2009; Parrot et al., 2007) reveal that, during an event, the same wave pattern is observed over a rather large area. However, MLR propagation properties cannot be clearly determined, principally because any observations at larger radial distances are extremely sparse, likely due to lack of spacecraft measurements with a sufficient frequency resolution.

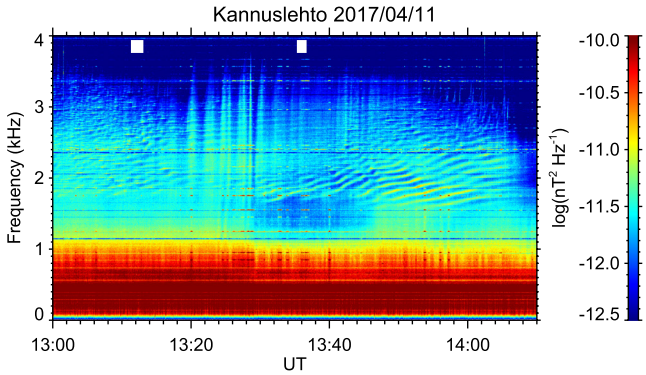

Figure 1. Frequency-time spectrogram of power spectral density of magnetic field fluctuations measured by the ground-based station Kannuslehto on 11 April 2017. Magnetospheric Line Radiation event lasting for nearly the entire plotted time interval can be seen. The white bars at the top mark the time intervals when Radiation Belt Storm Probes A high-resolution burst mode measurements were available.

We use continuous high-resolution burst mode wave data obtained by the Van Allen Probes spacecraft to systematically look for and analyze MLR events. Their occurrence and properties are analyzed, and the presence of an electrostatic wave with a frequency corresponding to the MLR frequency spacing is shown. The data set is described in Section 2. The obtained results are presented in Section 3 and discussed in Section 4. Finally, Section 5 contains a brief summary.

2. Data

The Van Allen Probes (formerly Radiation Belt Storm Probes (RBSP)) mission (2012–2019) consisted of two identical spacecraft with nearly the same low-inclination orbits. The perigee and apogee of the orbits were about 1.1 and 6 R_E, respectively. The spacecraft were generally within about 20° from the geomagnetic equator. Multicomponent electromagnetic wave measurements at frequencies up to 12 kHz were performed by the Waves instrument of the Electric and Magnetic Field Instrument Suite and Integrated Science (EMFISIS) suite (Kletzing et al., 2013). Survey mode spectra organized in 65 frequency bins do not have a sufficient frequency resolution to identify and analyze narrowband emissions such as MLR. Occasionally active continuous burst mode measurements are thus used in the present paper. These provide waveforms of all six electromagnetic field components sampled at 35 kHz over a duration of about 5.968 s, followed by about 0.032 s long data gap. The total duration of a single burst mode interval is thus about 6 s. However, the burst mode is at times active for several consecutive intervals, resulting in longer, nearly continuous burst mode data.

Considering that the identification of MLR events generally requires longer time intervals to properly distinguish the events, only data formed by at least 15 consecutive burst mode subintervals (i.e., at least 90 s nearly continuous burst mode data) are considered. Altogether, as many as 6,803 such time intervals occurred during the entire duration of the Van Allen Probes mission. For each of them, we plotted a frequency-time spectrogram of the power spectral density of magnetic field fluctuations and visually checked for the presence of MLR. Altogether, 15 MLR events were identified. This would correspond to an occurrence rate of about 0.2%, if the analyzed set of measurements was randomly distributed. However, this is hardly the case, as the burst mode time intervals are acquired primarily at large L-shells (Němec et al., 2022). Indeed, nearly 70% of the analyzed burst mode time intervals were measured at $L > 4$ and nearly 40% at $L > 5$.

In addition to the EMFISIS electromagnetic wave measurements, local plasma number density data obtained from the upper hybrid frequency (Kurth et al., 2015) are used. Finally, simultaneous two-component horizontal magnetic field measurements with a sampling frequency of 78,125 Hz performed by the ground-based station Kannuslehto (67.74°N, 26.27°E, $L \approx 5.5$) operated by the Sodankylä Geophysical Observatory in Finland are used for one of the events (Manninen, 2005).

3. Results

One of the identified MLR events is observed not only by the Van Allen Probes spacecraft but also by the Kannuslehto station. This is advantageous, as the long-lasting ground-based observations can reveal the temporal evolution and duration of the event, which is not possible using spacecraft measurements with a very limited duration. The corresponding frequency-time spectrogram measured by the Kannuslehto station is shown in Figure 1. The data were obtained on 11 April 2017. The MLR event lasts for essentially the entire plotted time interval (13:00–14:10 UT), that is, more than 1 hour. Note that magnetic local time (MLT) of Kannuslehto is about +3 hr from UT. Also note that the fixed-frequency lines are due to PLHR and the result of filtering them out of the spectrum, and they are not part of the MLR spectrum. The white bars at the top of the plot mark the two subintervals for which the burst mode data measured by RBSP A are available. The spacecraft MLTs during these two time intervals are about 16.1 and 16.6 hr, respectively, that is, similar to the MLT of Kannuslehto. However, detailed frequency-time spectrograms plotted for these two time intervals reveal that the MLR event is observed by the RBSP A spacecraft only during the first time interval.

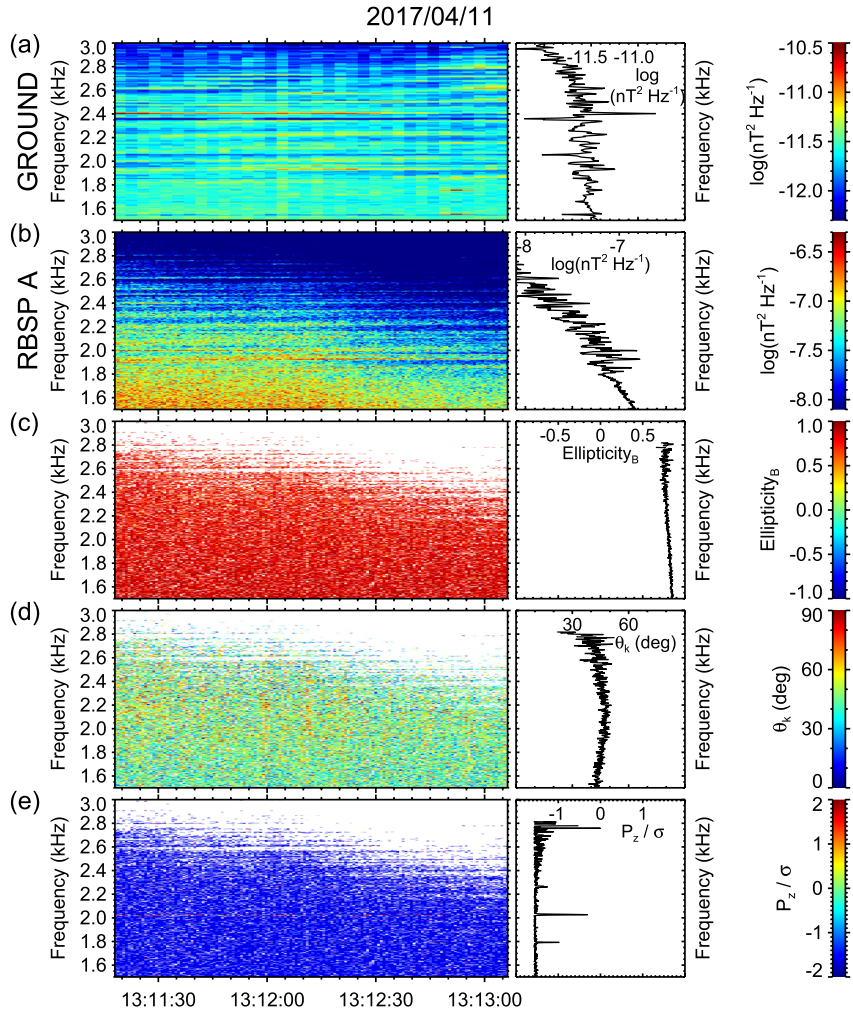

Figure 2. Data obtained on 11 April 2017 during the time interval marked by the first white bar in Figure 1. The left column shows frequency-time plots and the right column shows the corresponding frequency dependences (i.e., averaged over the time). (a) Power spectral density of magnetic field fluctuations measured by the Kannuslehto station. (b) Power spectral density of magnetic field fluctuations measured by Radiation Belt Storm Probes (RBSP) A. (c) Ellipticity of magnetic field fluctuations determined from the RBSP A measurements. (d) Wave normal angle determined from RBSP A measurements. (e) Parallel component of the Poynting vector normalized by the standard deviation (σ) determined from the RBSP A measurements.

Frequency-time plots and frequency dependences corresponding to the Kannuslehto and RBSP A measurements during the first time interval marked in Figure 1 are shown in Figure 2. The left column shows frequency-time plots of individual wave properties, and the right column shows the corresponding frequency dependences (i.e., the frequency-time plots averaged over time). Figures 2a and 2b show the power spectral density of magnetic field fluctuations measured by the Kannuslehto station and by RBSP A, respectively. Figures 2c–2e depict selected wave properties determined using the multicomponent RBSP A measurements. The signed ellipticity of magnetic field fluctuations and the wave normal angle calculated using the singular value decomposition method (Santolík et al., 2002, 2003) are shown in Figures 2c and 2d, respectively. The obtained ellipticity values close to 1 correspond to right-handed nearly circularly polarized waves. The wave normal angles are about 40°. Figure 2e depicts the values of the parallel component of the Poynting flux normalized by its experimental uncertainty (Santolík et al., 2001). The obtained negative values correspond to the wave propagation opposite to the ambient magnetic field, that is, southward. Given that the RBSP A spacecraft is, at the time of the observation, located at negative magnetic latitudes, this corresponds to the wave propagation away from the magnetic equator.

The locations of the RBSP A spacecraft and the Kannuslehto station at the time of the observation are depicted in Figure 3a. Note that as they are located essentially in the same magnetic meridian (MLT of 16.1–16.6 and

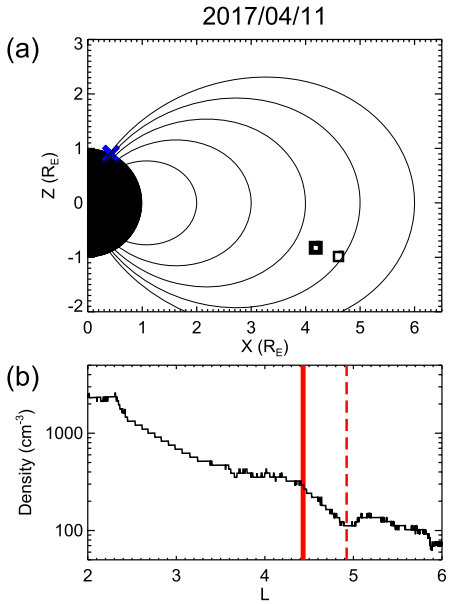

Figure 3. (a) Locations of the Radiation Belt Storm Probes (RBSP) A spacecraft at the time of the event from Figure 1 are shown by the black squares. The location at the time marked by the first white bar in Figure 1, corresponding to the time from Figure 2 when the event was observed by the spacecraft, is shown by the thicker square. The location at the time marked by the second white bar in Figure 1, when the event was no longer observed by the spacecraft, is shown by the thinner square. The blue cross shows the location of the Kannuslehto station. Magnetic field lines are shown by the black curves. (b) In situ measured plasma number density as a function of L-shell. The L-shells corresponding to the two time intervals with the RBSP A burst mode data available are shown by the solid and dashed vertical red lines, respectively.

16.2–16.6 hr, respectively), only the meridional view is shown. The location of the Kannuslehto station is shown by the blue cross. The location of the RBSP A spacecraft at the time of the measurements from Figure 2 is shown by the thick square symbol. The location of the RBSP A spacecraft at the second time interval marked in Figure 1, when the MLR event is no longer detected by the spacecraft, is shown by the thinner square symbol. The thin curves show the magnetic field lines. It can be seen that the spacecraft L-shell at the second time interval is about 0.5 larger than during the first time interval. Figure 3b shows the in-situ measured plasma densities around the observation time as a function of L-shell. The solid and dashed vertical red lines mark the L-shells of the RBSP spacecraft at the times corresponding to the thick and thinner square symbols, respectively. Although the density profile lacks a sharp well-pronounced plasmapause, a plasmapause-like density gradient is seen between L-shells of about 4.5 and 5.0. During the second time interval, when the MLR event is no longer observable, the spacecraft is located outside of the density gradient, and the density is thus significantly lower than during the first time interval (by a factor of about 3). Therefore, the event does not extend beyond the high-density plasmasphere region.

Locations of the 15 identified MLR events projected along the magnetic field lines to the equatorial plane are shown in Figure 4a. It can be seen that the events are observed in a wide interval of L-shells between 2 and 6, but mostly at L-shells between about 4 and 5, primarily on the dayside. Frequencies of the identified MLR events are analyzed in Figure 4b. For each frequency, the number of MLR events spanning that particular frequency is depicted. The event frequencies are mostly between 1 and 4 kHz, but some may extend up to about 7 kHz.

Multicomponent wave observations of MLR events at larger radial distances provide a unique opportunity to analyze the wave propagation closer to the tentative source regions than ever possible before. For each of the events, we manually select the corresponding frequency-time interval. Additionally, an event-specific intensity threshold is used to select only elementary frequency-time subintervals corresponding to the event line structure. Finally, the median value of a given propagation parameter is calculated in order to get a single propagation parameter value for each of the events. The results obtained for the polar angles of the wave and Poynting vector directions are shown in Figure 5.

The format of Figures 5a and 5b is the same. Each square symbol corresponds to one MLR event. The abscissa shows the geomagnetic latitude, and the ordinate shows the polar angles of the wave and Poynting vector directions. The three events observed at L-shells lower than three are shown in blue. The wave normal angles depicted in Figure 5a are mostly less than 45°, and they do not exhibit any clear dependence on the geomagnetic latitude. On

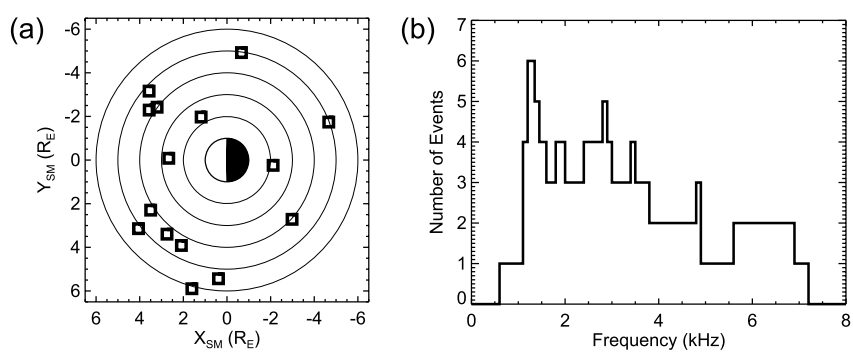

Figure 4. (a) Locations of identified magnetospheric line radiation events projected along dipolar magnetic field lines to the equatorial plane. (b) Histogram of ranges of frequencies over which the identified events are seen.

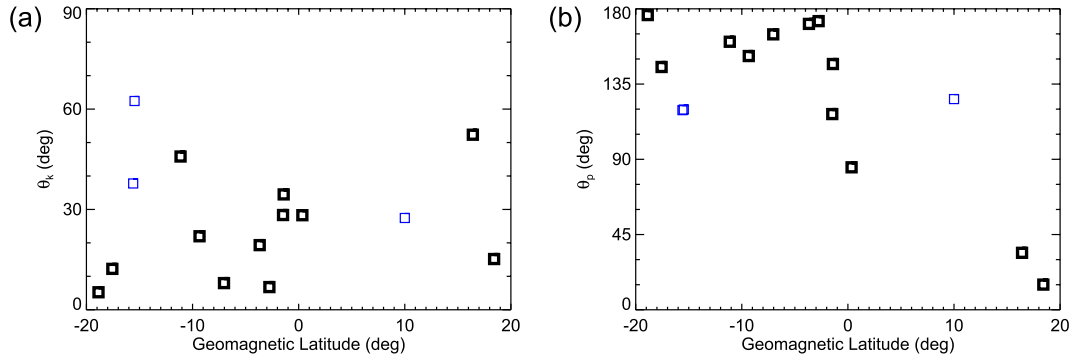

Figure 5. Median propagation parameters of individual events. The events observed at $L < 3$ are shown by the blue squares, all other events are shown by the black squares. (a) Wave normal angle as a function of the geomagnetic latitude. (b) Polar angle of the Poynting vector as a function of the geomagnetic latitude.

the other hand, the Poynting vector directions, which allow us to distinguish the propagation along/opposite the ambient magnetic field, reveal a difference between the propagation directions northward and southward of the geomagnetic equator. While the polar angles of Poynting vector directions southward of the geomagnetic equator tend to be larger than 135°, corresponding to the propagation opposite to the ambient magnetic field, the polar angles of Poynting vector directions northward of the geomagnetic equator tend to be lower than 45°, corresponding to the propagation along the ambient magnetic field. This corresponds to the wave propagation away from the geomagnetic equator, indicating that the wave source is located at the equator. Note that the polar angle of the Poynting vector of the event observed at the geomagnetic latitude of about 10° is close to about 130°, corresponding to the southward wave propagation. This event apparently violates the aforementioned trend of propagation away from the geomagnetic equator. However, it is noteworthy that this particular event was observed at a rather low L-shell ($L = 2.1$). The events at lower L-shells possibly do not propagate directly from the source, but they might have undergone a magnetospheric reflection. This may possibly explain this particular event, similarly as, for example, in the case of quasiperiodic emissions (Němec et al., 2014) and plasmaspheric hiss (Bortnik et al., 2008; Hartley et al., 2018).

Previously available ground-based and low-altitude spacecraft observations of MLR events did not allow an experimental confirmation/rejection of the hypothesis of the events being formed due to the interaction with a wave with a frequency corresponding to the frequency spacing (Němec, Parrot, & Santolík, 2012). The reason is that this hypothetical wave would not propagate down to low altitudes. On the other hand, the Van Allen Probes observations at larger radial distances might be eventually suitable for its detection. We thus check for the presence of a wave at a frequency corresponding to the MLR frequency spacing in all the 15 analyzed MLR events. Both the power spectral density of magnetic field fluctuations and the power spectral density of electric field fluctuations are investigated for this purpose. While no particular signature is found in the magnetic field data, electric field data for three of the events reveal increased wave intensities at the corresponding frequencies. An example of one such event is shown in Figure 6.

Figure 6a shows a frequency-time spectrogram of the power spectral density of electric field fluctuations in the frequency-time interval corresponding to the MLR event measured by RBSP B on 29 April 2018 between 15:36 and 15:47 UT (MLT about 5.4–5.6 hr). The frequency spectrum calculated over the time interval marked by the vertical white dashed lines, when the event line structure is particularly well pronounced, is shown on the right-hand side. The four horizontal blue lines mark the frequencies of the most intense spectral peaks (1,337.0, 1,381.5, 1,426, and 1,470.5 Hz). Figure 6b uses the same format as Figure 6a but with an expanded frequency axis to show the power spectral density of electric field fluctuations at lower frequencies, only up to 250 Hz. An increased intensity at the frequency of about 45 Hz, corresponding to the frequency spacing of the MLR event, can be seen. The frequency spread of this spectral peak at 45 Hz is also similar to the frequency bandwidth of the individual MLR lines, which is about 10–20 Hz. Moreover, the time variation of the wave intensity at a frequency of about 45 Hz corresponds to the time variation of the wave intensity at MLR frequencies. Specifically, it peaks between about 15:36 and 15:39 UT, followed by a gap between about 15:39 and 15:42 UT, with a subsequent peak between about 15:42 and 15:44 UT, and only comparatively low intensities afterward. The corresponding frequency spectrum obtained for the time interval marked by the white vertical dashed lines is

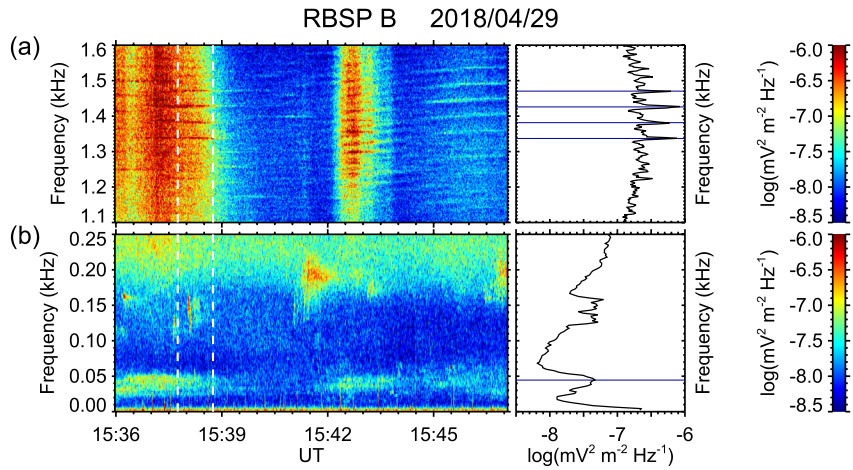

Figure 6. Data obtained by Radiation Belt Storm Probes B on 29 April 2018. The left column shows frequency-time spectrograms of power spectral density of electric field fluctuations and the right column shows the corresponding frequency spectra. (a) Frequencies between 1,100 and 1,600 Hz, where the Magnetospheric Line Radiation (MLR) event is observed. (b) Frequencies between 0 and 250 Hz, revealing a wave at a frequency corresponding to the frequency spacing of the MLR event.

shown on the right-hand side. The frequency of the spectral peak, marked by the horizontal blue line, corresponds to the frequency spacing of the spectral peaks in Figure 6a (44.5 Hz). Note that the local proton cyclotron frequency and the lower hybrid frequency are about 4 and 172 Hz, respectively. The observed wave frequency thus does not correspond to either of them. The observed wave might possibly be a lower hybrid drift wave (Liu et al., 2021; Ouyang et al., 2022), which occurs at times at frequencies well below the lower hybrid frequency (Blecki et al., 1988; Carter et al., 2002).

4. Discussion

MLR is not yet a well understood phenomenon occurring in the Earth's inner magnetosphere. The identification of the line structure of MLR events requires a sufficiently high frequency resolution, that is, a frequency resolution generally better than the frequency separation of MLR spectral lines (about 100 Hz). Such high-resolution measurements are only sporadically performed by spacecraft operating at larger radial distances. Consequently, most MLR observations up to now have been performed either by ground-based or low-altitude spacecraft. Although such observations are very beneficial, they are intrinsically affected by the magnetospheric wave propagation from the hypothetical source region to the observation point and, in the case of a ground-based station, also by the propagation in the Earth-ionosphere waveguide. This complicates the mapping of the event occurrence and, at the same time, prevents the identification of possible low frequency waves responsible for the MLR frequency modulation (Němec, Parrot, & Santolík, 2012). The high-resolution multicomponent measurements performed by the EMFISIS Waves instruments on board the Van Allen Probes close to the geomagnetic equator at larger radial distances overcome this issue. Limiting the analysis to only reasonably long (at least 90 s) burst mode data intervals reduces considerably the amount of data to be analyzed. However, as many as 15 MLR events are identified in total, which is sufficient to reveal their basic properties.

The events occur primarily on the dayside, with only three events identified during the nighttime hours. This seems to be quite consistent with the event occurrence as observed by the low-altitude spacecraft, which was found to be about 1.4–1.7 times higher during the day than during the night (Bezděková et al., 2015; Němec, Parrot, et al., 2009). The frequencies of the RBSP events also correspond to the low-altitude spacecraft observations. Given that MLR is observed mainly in the daytime magnetosphere, it is tempting to relate its occurrence to specific solar wind parameters. Although the set of only 15 events, which are analyzed in the present paper, is insufficient for such a study, Bezděková et al. (2015) found, based on more frequent MLR observations by the DEMETER spacecraft, that MLR occurs more often after periods of enhanced geomagnetic activity, being statistically related to specific solar wind parameters. In particular, the mean solar wind speed was shown to be about 50 km/s above average approximately 1 day before MLR events, the mean proton density was found

to decrease around the times of the events, and the primarily negative interplanetary magnetic field B_z before the events sharply increases at the event times. We note, however, that all these variations are rather small as compared to the global variability of the solar wind parameters, and they are identifiable and statistically significant only due to a large number of analyzed events (more than 1,000).

Most events are observed at L-shells between about 4 and 5, that is, not too far from a typical plasmapause location. The low number of events at $L < 4$ is possibly related to the poor burst mode data coverage of that region. This might also explain why the perceived event occurrence of about 0.2% is much lower than the event occurrence of about 2% determined using low-altitude spacecraft data (Bezděková et al., 2015; Němec, Parrot, et al., 2009). Additionally, the events at lower altitudes are possibly further spread in space due to unducted propagation and ionospheric reflections, similar to quasiperiodic emissions in the same frequency range (Hanzelka et al., 2017; Hayosh et al., 2016). The in-situ measured densities at the times of the events range between about 60 and 2,350 cm^{-3}, with an average value of about 580 cm^{-3}. Out of the eight events for which the plasmapause is well identifiable, seven events are observed inside the plasmasphere. The density profiles in the remaining seven events are rather smooth, similar to the situation depicted in Figure 3, and the plasmapause location cannot be determined. The importance of the plasma number densities for the event occurrence is further indicated by the analysis of conjugate observations performed by the Kannuslehto station. While the ground-based station observed the event continuously for the entire analyzed time interval, RBSP A observed the event only during the first burst mode interval, when it was located in a region with a comparatively larger density. The MLR event was no longer observed by RBSP A during the second burst mode interval when the spacecraft L-shell was by about 0.5 larger and the local plasma density was lower (about 300 vs. 100 cm^{-3}, respectively).

Detailed wave analysis using multicomponent wave measurements reveals that the waves observed at $L > 3$ propagate at oblique wave normals away from the geomagnetic equator. This represents a strong experimental indication that the waves are indeed generated at the equatorial region at larger radial distances, as has been suspected but not really demonstrated so far. The propagation of events at lower L-shells may be more complicated, with one of the identified events even propagating toward the geomagnetic equator. This can be, however, likely explained by the magnetospheric reflection of the waves and their subsequent propagation back to the equator at lower L-shells. The viability of such a propagation scheme for the waves of the studied frequencies has been demonstrated by raytracing calculations (Němec et al., 2014).

The origin of the frequency modulation of MLR events is still unknown. Němec, Parrot, and Santolík (2012) showed that individual lines cannot be explained as harmonics of the base frequency equal to the frequency spacing. They suggested that the frequency modulation may result from an interaction between a wave of a carrier frequency and an additional wave with a frequency equal to the frequency spacing. However, such a hypothetical modulating wave would not propagate to low altitudes and it is thus in principle not detectable by ground-based stations/low-altitude spacecraft even if it existed. Nevertheless, the RBSP observations performed close to the equatorial plane at larger radial distances indeed reveal the existence of such a wave in three of the analyzed events. It is observed exclusively in the electric field data, with no magnetic field counterpart, and can be thus considered as (quasi-)electrostatic. In all three cases, the wave frequency corresponds well to the observed MLR frequency spacing, and in the presented event it also exhibits a very similar time dependence. The possibility of a whistler wave modulation by an electrostatic wave was considered by Kulkarni and Das (1975), who suggested that the trapping of particles by the electrostatic wave could result in a series of resonances for the whistler-mode, inducing the wave growth at a discrete set of frequencies. Alternatively, one may consider some kind of a parametric interaction resulting in a periodic sideband structure (Main & Sotnikov, 2020; Sotnikov et al., 1991). Note, nevertheless, that the bicoherence analysis (Graham et al., 2014; Lagoutte et al., 1989) does not reveal any significant wave-wave interaction taking place. This may be due to the observations taking place slightly away from the interaction region, where the wave phases are no more strictly interlocked. Alternatively, one may consider the plasma effects on the performed electric field measurements, possibly biasing the phase values (Hartley et al., 2022).

5. Conclusions

We used multicomponent continuous burst mode data obtained by the EMFISIS Waves instrument onboard the Van Allen Probes spacecraft to systematically search for and investigate MLR events. Such observations at larger radial distances close to the geomagnetic equator are rather unique, as most previous MLR observations come

from low-altitude satellites and ground-based stations. Altogether, 15 MLR events were analyzed. Most of them occurred on the dayside at frequencies between about 1 and 5 kHz. Detailed wave analysis revealed the propagation at oblique wave normal angles away from the equatorial plane, suggesting that MLR is indeed generated close to the geomagnetic equator. One of the events was simultaneously observed also by the ground-based Kannuslehto station in Finland. While the event was readily observable by the station for a longer time period, it was detected by RBSP only in one of the two intervals with the burst mode coverage. This imposes limits on the spatial extent of the event, which does not seem to extend beyond the dense plasmasphere region. Finally, electrostatic waves with frequencies corresponding to the MLR frequency spacing were identified in three events, likely linked to the event formation mechanism.

Data Availability Statement

Van Allen Probes A and B data used in this paper can be accessed from the websites https://spdf.gsfc.nasa.gov/pub/data/rbsp/rbspa/l2/emfisis/wfr/waveform/ and https://spdf.gsfc.nasa.gov/pub/data/rbsp/rbspb/l2/emfisis/wfr/waveform/. The respective SPASE resource descriptions can be found at https://hpde.io/NASA/NumericalData/RBSP/A/EMFISIS/WFR/L2/WAVEFORM/PT6S and https://hpde.io/NASA/NumericalData/RBSP/B/EMFISIS/WFR/L2/WAVEFORM/PT6S, respectively (Kletzing, 2022a, 2022b).

Acknowledgments
F. N. and O. S. acknowledge the support of GACR Grant 21-01813S and MSMT Grant LUAUS23152.

References

Bell, T. F., Luette, J. P., & Inan, U. S. (1982). ISEE 1 observations of VLF line radiation in the Earth's magnetosphere. *Journal of Geophysical Research*, *87*(A5), 3530–3536. https://doi.org/10.1029/JA087iA05p03530

Bezděková, B., Němec, F., Parrot, M., Hajoš, M., Záhlava, J., & Santolík, O. (2019). Dependence of properties of magnetospheric line radiation and quasiperiodic emissions on solar wind parameters and geomagnetic activity. *Journal of Geophysical Research: Space Physics*, *124*, 2552–2568. https://doi.org/10.1029/2018JA026378

Bezděková, B., Němec, F., Parrot, M., Santolík, O., & Kruparova, O. (2015). Magnetospheric line radiation: 6.5 years of observations by the DEMETER spacecraft. *Journal of Geophysical Research: Space Physics*, *120*(11), 9442–9456. https://doi.org/10.1002/2015JA021246

Blecki, J., Kossacki, K., Popielawska, B., Klimov, S. I., Romanov, S. A., Savin, S. P., & Zeleny, L. M. (1988). ELF plasma waves associated with plasma jets near the Earth magnetopause as observed by Prognoz-8. *Physica Scripta*, *37*(4), 623–631. https://doi.org/10.1088/0031-8949/37/4/022

Bortnik, J., Thorne, R. M., & Meredith, N. P. (2008). The unexpected origin of plasmaspheric hiss from discrete chorus emissions. *Nature*, *452*(7183), 62–66. https://doi.org/10.1038/nature06741

Carter, T. A., Yamada, M., Ji, H., Kulsrud, R. M., & Trintchouk, F. (2002). Experimental study of lower-hybrid drift turbulence in a reconnecting current sheet. *Physics of Plasmas*, *9*(8), 3272–3288. https://doi.org/10.1063/1.1494433

Graham, D. B., Malaspina, D. M., & Cairns, I. H. (2014). Applying bicoherence analysis to spacecraft observations of Langmuir waves. *Geophysical Research Letters*, *41*(5), 1367–1374. https://doi.org/10.1002/2014GL059565

Hanzelka, M., Santolík, O., Hajoš, M., Němec, F., & Parrot, M. (2017). Observation of ionospherically reflected quasiperiodic emissions by the DEMETER spacecraft. *Geophysical Research Letters*, *44*(17), 8721–8729. https://doi.org/10.1002/2017GL074883

Hartley, D. P., Christopher, I. W., Kletzing, C. A., Kurth, W. S., Santolík, O., Kolmašová, I., et al. (2022). Quantifying the sheath impedance of the electric double probe instrument on the Van Allen Probes. *Journal of Geophysical Research: Space Physics*, *127*(5), e2022JA030369. https://doi.org/10.1029/2022JA030369

Hartley, D. P., Kletzing, C. A., Santolík, O., Chen, L., & Horne, R. B. (2018). Statistical properties of plasmaspheric hiss from Van Allen Probes observations. *Journal of Geophysical Research: Space Physics*, *123*(4), 2605–2619. https://doi.org/10.1002/2017JA024593

Hayosh, M., Němec, F., Santolík, O., & Parrot, M. (2016). Propagation properties of quasiperiodic VLF emissions observed by the DEMETER spacecraft. *Geophysical Research Letters*, *43*(3), 1007–1014. https://doi.org/10.1002/2015GL067373

Kletzing, C. A. (2022a). Van Allen Probe A WFR waveform data [Dataset]. NASA Space Physics Data Facility. https://doi.org/10.48322/13vc-c837

Kletzing, C. A. (2022b). Van Allen Probe B WFR waveform data [Dataset]. NASA Space Physics Data Facility. https://doi.org/10.48322/mf9b-6r41

Kletzing, C. A., Kurth, W. S., Acuna, M., MacDowall, R. J., Torbert, R. B., Averkamp, T., et al. (2013). The electric and magnetic field instrument suite and integrated science (EMFISIS) on RBSP. *Space Science Reviews*, *179*(1–4), 127–181. https://doi.org/10.1007/s11214-013-9993-6

Kulkarni, V. H., & Das, A. C. (1975). Effect of trapped particles in an electrostatic wave on the whistler mode. *Physics Letters A*, *53*(1), 94–96. https://doi.org/10.1016/0375-9601(75)90361-8

Kurth, W. S., Pascuale, S. D., Faden, J. B., Kletzing, C. A., Hospodarsky, G. B., Thaller, S., & Wygant, J. R. (2015). Electron densities inferred from plasma wave spectra obtained by the Waves instrument on Van Allen Probes. *Journal of Geophysical Research: Space Physics*, *120*(2), 904–914. https://doi.org/10.1002/2014JA020857

Lagoutte, D., Lefeuvre, F., & Hanasz, J. (1989). Application of bicoherence analysis in study of wave interactions in space plasma. *Journal of Geophysical Research*, *94*(A1), 435–442. https://doi.org/10.1029/JA094iA01p00435

Liu, X., Chen, L., & Ma, Q. (2021). A statistical study of lower hybrid waves in the Earth's magnetosphere by Van Allen Probes. *Geophysical Research Letters*, *48*(10), e2021GL093168. https://doi.org/10.1029/2021GL093168

Main, D., & Sotnikov, V. (2020). Parametric interaction between ELF and VLF waves: 3D LSP simulation results. *Physics of Plasmas*, *27*(2), 022304. https://doi.org/10.1063/1.5126675

Manninen, J. (2005). In *Some aspects of ELF-VLF emissions in geophysical research* (pp. 85–110). Sodankylä Geophysical Observatory Publications.

Matthews, J. P., & Yearby, K. (1981). Magnetospheric VLF line radiation observed at Halley, Antarctica. *Planetary and Space Science*, *29*(1), 97–106. https://doi.org/10.1016/0032-0633(81)90142-2

Němec, F., Parrot, M., & Santolík, O. (2012). Detailed properties of magnetospheric line radiation events observed by the DEMETER spacecraft. *Journal of Geophysical Research*, *117*(A5), A05210. https://doi.org/10.1029/2012JA017517

Němec, F., Parrot, M., Santolík, O., Rodger, C. J., Rycroft, M. J., Hayosh, M., et al. (2009). Survey of magnetospheric line radiation events observed by the DEMETER spacecraft. *Journal of Geophysical Research*, *114*(A5), A05203. https://doi.org/10.1029/2008JA014016

Němec, F., Pickett, J. S., & Santolík, O. (2014). Multi-spacecraft Cluster observations of quasi-periodic emissions close to the geomagnetic equator. *Journal of Geophysical Research: Space Physics*, *119*(11), 9101–9112. https://doi.org/10.1002/2014JA020321

Němec, F., Raita, T., Parrot, M., Santolík, O., & Turunen, T. (2009). Conjugate observations on board a satellite and on the ground of a remarkable MLR-like event. *Geophysical Research Letters*, *36*(22), L22103. https://doi.org/10.1029/2009GL040974

Němec, F., Santolík, O., Hospodarsky, G. B., Kurth, W. S., & Kletzing, C. (2022). Power line harmonic radiation observed by the Van Allen Probes spacecraft. *Journal of Geophysical Research: Space Physics*, *127*(6), e2022JA030320. https://doi.org/10.1029/2022JA030320

Němec, F., Santolík, O., Parrot, M., & Berthelier, J. J. (2006). Power line harmonic radiation (PLHR) observed by the DEMETER spacecraft. *Journal of Geophysical Research*, *111*(A4), A04308. https://doi.org/10.1029/2005JA011480

Němec, F., Santolík, O., Parrot, M., & Berthelier, J. J. (2007a). Comparison of magnetospheric line radiation and power line harmonic radiation: A systematic survey using the DEMETER spacecraft. *Journal of Geophysical Research*, *112*(A4), A04301. https://doi.org/10.1029/2006JA012134

Němec, F., Santolík, O., Parrot, M., & Berthelier, J. J. (2007b). Power line harmonic radiation: A systematic study using DEMETER spacecraft. *Advances in Space Research*, *40*(3), 398–403. https://doi.org/10.1016/j.asr.2007.01.074

Němec, F., Santolík, O., Parrot, M., & Bortnik, J. (2008). Power line harmonic radiation observed by satellite: Properties and propagation through the ionosphere. *Journal of Geophysical Research*, *113*(A8), A08317. https://doi.org/10.1029/2008JA013184

Němec, F., Santolík, O., Parrot, M., & Pickett, J. S. (2012). Magnetospheric line radiation event observed simultaneously on board Cluster 1, Cluster 2 and DEMETER spacecraft. *Geophysical Research Letters*, *39*(18), L18103. https://doi.org/10.1012/GL053132

Ouyang, Z., Li, H., Yuan, Z., Yu, X., Tang, R., & Deng, X. (2022). In situ observations of lower hybrid drift waves at the inner edge of the ring current by the Van Allen Probe-A. *Geophysical Research Letters*, *49*(21), e2022GL100485. https://doi.org/10.1029/2022GL100485

Parrot, M., Manninen, J., Santolik, O., Nemec, F., Turunen, T., Raita, T., & Macusova, E. (2007). Simultaneous observation on board a satellite and on the ground of large-scale magnetospheric line radiation. *Geophysical Research Letters*, *34*(19), L19102. https://doi.org/10.1029/2007GL030630

Rodger, C. J., Clilverd, M. A., Yearby, K., & Smith, A. J. (2000a). Is magnetospheric line radiation man-made? *Journal of Geophysical Research*, *105*(A7), 15981–15990. https://doi.org/10.1029/1999JA000413

Rodger, C. J., Clilverd, M. A., Yearby, K. H., & Smith, A. J. (1999). Magnetospheric line radiation observations at Halley, Antarctica. *Journal of Geophysical Research*, *104*(A8), 17441–17447. https://doi.org/10.1029/1999JA900153

Rodger, C. J., Clilverd, M. A., Yearby, K. H., & Smith, A. J. (2000b). Temporal properties of magnetospheric line radiation. *Journal of Geophysical Research*, *105*(A1), 329–336. https://doi.org/10.1029/1999JA900420

Rodger, C. J., Thomson, N. R., & Dowden, R. L. (1995). VLF line radiation observed by satellite. *Journal of Geophysical Research*, *100*(A4), 5681–5689. https://doi.org/10.1029/94JA02865

Santolík, O., Lefeuvre, F., Parrot, M., & Rauch, J. L. (2001). Complete wave-vector directions of electromagnetic emissions: Application to INTERBALL-2 measurements in the night-side auroral zone. *Journal of Geophysical Research*, *106*(A7), 13191–13201. https://doi.org/10.1029/2000ja000275

Santolík, O., Parrot, M., & Lefeuvre, F. (2003). Singuar value decomposition methods for wave propagation analysis. *Radio Science*, *38*(1). https://doi.org/10.1029/2000RS002523

Santolík, O., Pickett, J. S., Gurnett, D. A., & Storey, L. R. O. (2002). Magnetic component of narrowband ion cyclotron waves in the auroral zone. *Journal of Geophysical Research*, *107*(A12), SMP17-21–SMP17-14. https://doi.org/10.1029/2001JA000146

Sotnikov, V. I., Fiala, V., Lefeuvre, F., Lagoutte, D., & Mogilevsky, M. (1991). Excitation of sidebands due to nonlinear coupling between a VLF transmitter signal and natural ELF emission. *Journal of Geophysical Research*, *96*(A7), 11363–11369. https://doi.org/10.1029/91JA00695